Asociación Argentina
de Mecánica Computacional

Mecánica Computacional Vol XXVIII, págs. 1579-1592 (artículo completo)
Cristian García Bauza, Pablo Lotito, Lisandro Parente, Marcelo Vénere (Eds.)
Tandil, Argentina, 3-6 Noviembre 2009

EVALUATION OF SLIP BOUNDARY CONDITION WITH RADIAL BASIS FUNCTION FOR IMPLEMENTATION IN BOUNDARY ELEMENT METHODS

César Nieto[a], Mauricio Giraldo[a] and Henry Power[b]

[a]*Grupo de Energía y Termodinámica, Facultad de Ingeniería Mecánica, Universidad Pontificia Bolivariana, Circular 1 No. 73-34, Medellín, Colombia, cesar.nieto@correo.upb.edu.co, mauricio.giraldo@correo.upb.edu.co*

[b]*School of Mechanical, Materials and Manufacturing Engineering, the University of Nottingham, Nottingham, NG7 2RD, UK, henry.power@nottingham.ac.uk*

Keywords: Slip flow, Boundary integral formulation, Radial basis function.

Abstract. The slip flow regime emerges as a consequence of the characteristic length reduction in Micro Electro-Mechanical Systems (MEMS) that work with fluids (e.g. medical sample testing devices, drug delivery systems, micro heat exchangers and mixer, among others). The boundary condition imposed to account for slip flow when solving continuum based governing equations relates the wall and fluid velocity difference with the local shear rate projection in the tangential direction at the boundary. Several works have evaluated slip boundary conditions with diverse methods and approximations, in some cases misusing expressions derived for planar infinite surfaces aligned with coordinate axis, to analyse curved surfaces or corner flows. In this work, the creeping flow of a Newtonian fluid under linear slip boundary conditions is simulated applying the Boundary Element Method (BEM). Radial Basis Functions (RBF) are used to approximate the tangential shear rate projection in slip boundary conditions. Two types of interpolations schemes were implemented: a local interpolation and global interpolation. The first one evaluates the tangential shear rate from a finite set of points near the boundary nodes, while the second interpolation approach employs all nodes in the fluid domain (boundary and internal nodes). Two fluid flow problems are used to test the performance of the solution achieved: Couette and slit flow, both having analytical solutions to which the results obtained are compared. This implementation is also tested using three different RBF's, where the numerical results show that the Generalized Thin Plate Spline (GTPS) function combined with a global interpolation scheme has the least square norm error, below 1%, for both fluid flow problems tested and less computational effort than a similarly accurate local approximation.

1 INTRODUCTION

Microsystems Technology (MST) devices are widely used in life sciences and chemistry applications, and its potential uses extend to medical sample testing (Gad-el Hak, 2006b) and drug delivery systems (Kleinstreuer et al., 2008); gas and liquid heat exchangers (Shui et al., 2007; Giraldo et al., 2008) and chemical mixers (Bothe et al., 2006) for enhancement of heat and mass transfer rates; and fluid control and measurement (Alvarado et al., 2009) devices. Micro heat exchangers and mixers are currently used for steam gas reforming to produce alternative fuels (Tonkovich et al., 2004), nuclear resources exploiting (Li et al., 2006), micro integrated circuits cooling (Lee et al., 2004), micro fuel cells (Won Cha et al., 2004), among others.

When geometry devices are scaled down, the surface-to-volume ratio increases dramatically so that the surface related phenomena become increasingly dominant, e.g. micro heat exchangers and micro mixers present higher heat and mass transfer rates than macro systems of equal capacity (Hu and Li, 2007). Therefore, some new features emerges when mechanical structures are sufficiently small, and it becomes important to understand the various types of interactions that arises between the fluid flow constituents and the solid surfaces that contain it.

Different phenomena associated with surface-fluid interactions can be expected when the continuum assumption is close to being broken. For gases, four important effects appear: rarefaction, compressibility, viscous heating and thermal creep. In liquids, phenomena like wetting, adsorption and electrokinetics may be present (Karniadakis et al., 2005). However, in both liquids and gases, a phenomenum known as the slip flow regime emerges as a consequence of an insufficient number of molecules in the sampling region (Thompson and Troian, 1997), affecting the momentum transport at solid-fluid interfaces compared with no slip type flows (i.e. macro scale flows).

So far, micro fluid flow behaviour has been studied under continuum (Gad-el Hak, 2006a) as well molecular approaches (Bird, 1994; Sadus, 1999), with the aim to characterize and optimize the operation of MST systems. In order for a fluid to be modelled as a continuum, all of its properties (i.e. kinematic, transport and thermodynamics properties) must be continuous; for that to be possible, enough molecules must be included compared to the length scale of the flow. In the case of gases, this premise is satisfied when the length scale based on transport properties is greater than $1\ \mu m\ (10^{-6}\ m)$; for liquids the length scale is based on transport properties and must be larger than $10\ nm\ (10^{-8}\ m)$ (Nguyen and Wereley, 2006). Appropriate velocity slip and temperature conditions at the wall surface must be used to employ continuum models to describe flow behaviour in microflow devices. Navier's slip boundary condition states that the relative tangential fluid velocity, u_t^f, with relation to wall velocity, U_t^w, is directly proportionally to the local shear rate projection in the tangential direction, $\dot{\gamma}_t$, as presented in equation (1). The proportionally constant is called slip length L_s, and represent the hypothetical distance at the wall needed to satisfy the no-slip flow condition (Nguyen and Wereley, 2006).

$$u_t^f - U_t^w = L_s \dot{\gamma}_t \tag{1}$$

$\dot{\gamma}_t$ being the local shear rate projection in the tangential direction defined as:

$$\dot{\gamma}_t = \left(\frac{\partial u_i}{\partial x_j} + \frac{\partial u_j}{\partial x_i} \right) n_j s_i \tag{2}$$

where n_i and s_i are respectively the i components of the normal and tangential vectors to a boundary surface. The main difficulty present when applying the previous boundary condition

is related to evaluation of tangential shear rate at solid-fluid interface. Linear boundary slip conditions have been applied to predict microflow behaviour in plane geometries with continuum governing equations. Attempts to apply this type of boundary conditions for curved surfaces have conducted to inappropriate microflow results due to mistreatment of mathematical models (see (Barber et al., 2004) for a compilation of those works).

Luo and Pozrikidis (2008) study the motion of spherical particles in infinite fluid and near a plane wall subjected to slip boundary conditions. The boundary integral formulation presented in this work takes advantage of the axial symmetry of the boundaries with respect to the axis that is normal to the wall and passes through the particle center, reducing the solution to a system of one-dimensional integral equations. The previous system of equations is valid for sphere and the zero-thickness disk, since the axisymmetry is lost as these particles tumble under the influence of a shear flow. Results for torque and drag over sphere show reduction associated to slip condition at those scales demonstrated the validity of numerical values when compared with analytical results.

Evaluation of slip fluid flow behaviour with boundary integral methods can be done in different forms: by solving a system of equations that couples both direct boundary integral equations for Stokes flow with boundary conditions for normal and tangential components for velocity and surface tractions in global coordinates (Nieto et al., 2009a); or by expressing tangential shear rate present in the slip boundary condition (1) in terms of tangential projection of surface tractions at fluid-solid interface and then solving the normal and tangential projection for boundary integral equations (Nieto et al., 2009b). In this paper, an alternative form of evaluating tangential shear rate with Radial Basis Functions (RBF) to implement the slip boundary condition in direct boundary integral equations is presented. Local and global interpolations are used to approach velocity gradients in shear rate expression allowing for the assessment of its accuracy through comparison against velocity profiles for the fluid flow problems solved. Analytical solutions for Couette and slit flow are used to test the numerical results obtained when taking into consideration different types of boundary conditions: the first has only Robin boundary conditions while the second is a mixed boundary condition problem (Robin, Dirichlet and Neumann).

This paper is divided as follows. Governing equations for Stokes flow are presented in section 2. In section 3 the boundary integral representation for governing equations are presented as well as the Boundary Element Method applied for its solution. A definition of the RBFs is presented in section 4, along with the methodology used to evaluate velocity gradients by means of RBF interpolation. The numerical results for Couette and slit flow are compared with analytical results through evaluation of least square norm error ($L2$ norm error) in section 5. Finally, conclusions regarding physical and mathematical considerations are given.

2 GOVERNING EQUATIONS

Fluid flow in micro scale devices usually happens at very low Reynolds number due to their small characteristic length scale. In these cases, the flow of an incompressible Newtonian viscous fluid can be modelled by the Stokes system of equations, which states a balance between the pressure and the viscous-shear forces. The Stokes system of equation can be written in dimensionless form as:

$$\frac{\partial u_i}{\partial x_i} = 0 \qquad \frac{\partial \sigma_{ij}}{\partial x_j} = 0 \tag{3}$$

where

$$\sigma_{ij} = -p\delta_{ij} + \left(\frac{\partial u_i}{\partial x_j} + \frac{\partial u_j}{\partial x_i}\right) \tag{4}$$

$\vec{u}$ being the velocity, p the pressure, and δ_{ij} the Kronecker delta. The characteristic terms for velocity, length scale and pressure in the case of the Couette flow are respectively ωr_i, r_i and $\mu\omega$, where r_i is the inner cylinder radii, ω is the angular velocity and μ is the fluid viscosity. For the slit flow the respective characteristic terms are hP_o/μ, h and P_o, where h is the slit height and P_o the inner reference pressure.

Boundary conditions are defined depending to the problem that is being solved. In the case of Couette flow (or the flow between concentric cylinders), the external cylinder is stationary while the internal one rotates at a constant angular dimensionless velocity of value 1. For slit flow (or fully developed flow between parallel plates), the superior and inferior surfaces are stationary, while at the entrance and exit the perpendicular velocities are made zero and the tractions are given only by a pressure difference between them. For the cases shown dimensionless pressure difference between entrance and exit, Δp equal to 1 is considered. Slip behaviour defined in equation (1) is considered by expressing local tangential shear rate in terms of vector surface traction defined in (5).

3 BOUNDARY INTEGRAL FORMULATION

The Stokes velocity field has the following direct integral representation formulae for an arbitrary point x in a closed domain Ω_i with surface S filled with a Newtonian fluid (Power and Wrobel, 1995):

$$c\left(x\right)\, u_i\left(x\right) - \int_S K_{ij}\left(x,y\right) u_j\left(y\right) dS_y + \int_S u_i^j\left(x,y\right) f_j\left(y\right) dS_y = 0 \tag{5}$$

where f is the vector surface tractions ($f_j(y) = \vec{\sigma}_{ij}\left(\vec{u},p\right) n_j$), and $c\left(x\right)$ is a constant dependent on the position of the source point. For internal points $c\left(x\right) = 1$ and for point at a smooth boundary $c\left(x\right) = 1/2$. The Stokeslet and the corresponding surface traction or Stresslet for two dimensions are given by:

$$u_i^j(x,y) = -\frac{1}{4\pi}\left[\ln\left(\frac{1}{r}\right)\delta_{ij} + \frac{\left(x_i - y_i\right)\left(x_j - y_j\right)}{r^2}\right] \tag{6}$$

$$K_{ij}\left(x,y\right) = -\frac{1}{\pi}\frac{\left(x_i - y_i\right)\left(x_j - y_j\right)\left(x_k - y_k\right) n_k\left(y\right)}{r^4} \tag{7}$$

being r the Euclidean distance between point x and y, $r = |x - y|$.

The Boundary Element Method can be used to solve the boundary integral equation (5) based on the discretization of the boundary surfaces. Discretization is performed in two stages: first is divided the surface of the problem S into N_e smaller elements or segments, S_j, leading to write integrals in equation (5) as:

$$c\left(x\right)\, u_i\left(x\right) - \sum_{j=1}^{N_e}\int_S K_{ij}\left(x,y\right) u_j\left(y\right) dS_{y_j} + \sum_{j=1}^{N_e}\int_S u_i^j\left(x,y\right) f_j\left(y\right) dS_{y_j} = 0 \tag{8}$$

Then, integral densities along the element are approximated by using interpolation functions on a given point along the element, call nodal points or nodes. In this way, equation (8) can be written in matrix form as:

$$c\left(x\right)\ u_i\left(x\right) - \sum_{j=1}^{N_e} \hat{H}_{ij} u_j - \sum_{j=1}^{N_e} G_{ij} f_j = 0 \tag{9}$$

being H_{ij} and G_{ij}, the matrix of influence coefficients, defined as follows:

$$\begin{aligned} \hat{H}_{ij} &= \int_S K_{ij}\left(x,y\right) dS_{y_j} \\ G_{ij} &= \int_S u_i^j\left(x,y\right)\ dS_{y_j} \end{aligned} \tag{10}$$

The left side of equation (9) can be written as follows:

$$\sum_{j=1}^{N} H_{ij}\,\mathbf{u} = \sum_{j=1}^{N} G_{ij}\,\mathbf{f} \tag{11}$$

being $\mathbf{u}$ and $\mathbf{f}$ velocity and traction vectors at evaluation points, and taking into account that H_{ij} is defined as:

$$H_{ij} = \begin{cases} \hat{H}_{ij} & when\ i \neq j \\ \hat{H}_{ij} + c_i & when\ i = j \end{cases} \tag{12}$$

When the discretised integral equation (11) for each boundary element are put together the final system of equations is written as:

$$\mathbf{HU} = \mathbf{GF} \tag{13}$$

Boundary conditions are introduced by moving columns of $\mathbf{H}$ and $\mathbf{G}$ from one side to other leading to:

$$\mathbf{AX} = \mathbf{B} \tag{14}$$

being $\mathbf{X}$ the vector of unknowns $\mathbf{u}$ and $\mathbf{f}$ at the boundary values and $\mathbf{B}$ the independent term that carries the known values over the bondary.

3.1 Integral Equation Discretizacion

Geometry discretization for numerical integration will be made with quadratic elements with the aim to improve evaluation of velocity and surface tractions at boundaries and to produce a more reliable micro scale flow behaviour. The interpolation scheme for a function $X(\varepsilon)$ is given by:

$$X\left(\varepsilon\right) = \psi_1\left(\varepsilon\right) X^{(1)} + \psi_2\left(\varepsilon\right) X^{(2)} + \psi_3\left(\varepsilon\right) X^{(3)} \tag{15}$$

where $X^{(1)}, X^{(2)}, X^{(3)}$ are the values of $X(\xi)$ on the three nodes of the element, being ξ the coordinates of the surface nodes when in equation (5) $x \in \Omega \rightarrow \xi \in S$. Then, the interpolation functions $\vec{\psi}$ are as follows:

$$\psi_1 = \tfrac{1}{2}\varepsilon\,(\varepsilon - 1)\,; \quad \psi_2 = (1-\varepsilon)\,(1+\varepsilon)\,; \quad \psi_3 = \tfrac{1}{2}\varepsilon\,(\varepsilon + 1) \tag{16}$$

defined in terms of an intrinsic coordinate ε, $-1 \leq \varepsilon \leq 1$. Standard Gaussian Quadrature is used to evaluate the final set of integrals resulting from applying the interpolation function (15). Telles' Transformation (Telles, 1987) and Rigid Body Motion (Brebbia and Dominguez, 1992) are used to avoid singularity present when integrating over the same element where the source point is located.

4 EVALUTION OF TANGENTIAL SHEAR RATE BY RADIAL BASIS FUNCTIONS

Radial Basis Functions (RBFs) have been used together with the BEM when non homogeneous terms are present in governing equations and domain integrals need to be evaluated after Green's second identity is used (Flórez and Power, 2001). The interpolation through RBF allows the expansion of the non homogeneous term in the governing equations avoiding the domain meshing. In this way, a set of boundary integrals is obtained for its solution through BEM after transforming the domain integrals by the interpolation performed with the RBFs. This approach has been successfully probed to evaluate several fluid flow problems concerning to non linear terms that depends on the derivatives of the velocity (Giraldo et al., 2008), (Giraldo et al., 2009).

Some features of the use of RBFs to approach the velocity field and its derivatives are related with the proficiency to compute interpolation from regular spaced or scattered data as well as the noise reduction during the interpolation process. The last characteristic can guarantee high accuracy of the evaluation of the first derivatives of the estimated function by interpolation evaluation function (Flórez and Power, 2001). In the present work, there is no presence of non homogeneous terms in governing equations since the direct integral formulae of Stokes flow equations are solved. Despite this, the slip condition imposed at the boundaries, requires calculating the derivatives of velocity. In such a way, the derivatives present in the tangential projection for the shear rate in the slip boundary condition (2), can be evaluated by RBF interpolation after expressing the velocity field at a domain point in terms of a function $f\,(x, y^m)$ and :

$$u_i = \sum_{m=1}^{p} f\,(x, y^m)\,(\beta_i^m) \tag{17}$$

or equivalently in matrix notation:

$$\{u_i\} = [F]\,\{\beta_i^m\} \tag{18}$$

$\{\beta_i^m\}$ being the interpolation coefficients vector to be determined by collocation on y^m $(m = 1, 2, 3, \ldots, p)$ points in the domain of interest where the derivative term is to be approximated. Then the velocity derivatives can be readily obtained by applying a differential operator to equation (17) in respect to x_j:

$$\frac{\partial u_i}{\partial x_j} = \sum_{m=1}^{p} \frac{\partial}{\partial x_j} f\,(x, y^m)\,(\beta_i^m) \tag{19}$$

or in matrix notation

$$\left\{\frac{\partial u_i}{\partial x_j}\right\} = \left[\frac{\partial F}{\partial x_j}\right]\{\beta_i^m\} \tag{20}$$

Inverting equation (18) and substituting the result into (20) yields:

$$\left\{\frac{\partial u_i}{\partial x_j}\right\} = \left[\frac{\partial F}{\partial x_j}\right][F]^{-1}\{u_i\} \tag{21}$$

thus relating the velocity derivatives to the values of the velocity on the collocation points. A wide variety of interpolating functions are available in the literature, the Generalized Thin Plate Spline (GTPS) being one of the most popular interpolating functions used:

$$f^m(x, y^m) = f(r(x, y^m)) = r^{2l-2}(x, y^m)\log(r(x, y^m)) + P_{l-1}(x) \tag{22}$$

where $P_{l-1}(x)$ is an augmentation polynomial of order $l-1$. Following Flórez and Power (2001) the parameter l is chosen to be equal to 2, with the aim of avoid numerical difficulties in the solution of the linear system of equations due to increase in the condition number of the resulting matrix. This leads to an augmentation polynomial of order $l-1=1$, $P_1(x)$, composed by the functions x_1, x_2 and 1. The GTPS is then expressed as:

$$f^m(x, y^m) = r^2(x, y^m)\log(r(x, y^m)) + P_1(x) \tag{23}$$

After expressing the velocity derivatives in terms of the velocity field through the implementation of RBF interpolation, the slip boundary condition is applied as follows. A first solution to the direct integral equation (5) is done under the no slip boundary condition. This solution is then used with both equation (23) and (21) to evaluate the velocity derivatives at collocation points. Two types of interpolation can be set: a local interpolation and a global interpolation. The first one is referred to a finite number of nodes limited by a fixed distance between the points over the surface and the nodes in the domain. The second approach refers to the use of all nodes both in the domain and the boundaries to evaluate the velocity derivatives over boundary nodes through . The detail of both approaches is presented in the following sections. The numerical results are compared with analytic results for velocity profiles of the fluid flow problems solved to verify its accuracy. Additionally, two different RBFs ($\sqrt{r+1}$, and, $1+r$) were tested and compared with the GTPS results to establish which interpolation function show better results to approximate the velocity derivatives on the boundary.

4.1 Local interpolation approach

The local approach refers to the interpolation of velocity derivatives by using just a few nodes close to the evaluation point at the surfaces subjected to the slip condition (i.e. solid-fluid interface). This is done in order to reduce the size of the RBF matrices, thus decreasing computational load. The first step in this iterative approach requires the evaluation of the velocity field under the no slip boundary condition. Then, the velocity derivatives for the source nodes in the direct boundary integral formulae (9) are evaluated using equation (21). The amount of nodes used in this approximation is established by the Euclidean distance r between collation points and the source point at the boundary. The linear slip boundary condition (1) is then used to evaluate the slip velocity at the solid-fluid interface by replacing the velocity derivatives approached through RBF interpolation. The velocity field and the velocity derivatives (as well as the slip velocity) are evaluated again under the new set of slip velocities over the surface.

The interpolation approach is performed individually over each surface node subject to the slip condition at each iteration. The process goes on until the velocity field stabilizes and the convergence criteria is achieved by comparing velocity values from actual iteration with previous one.

4.2 Global interpolation approach

As in the local interpolation, initial values for the velocity field are set through the solution of governing equations under the no slip boundary condition. Nevertheless, in the global approach all the domain nodes are used to relate both velocities and derivatives. Moreover the interpolation is performed over all the source points at the surface boundary while for the local approach N_b iterations are required; being N_b the number of nodes in boundary under slip condition. The velocity derivatives at boundary nodes are then applied to solve the velocity field under the slip boundary condition. The process finishes when the convergence criteria is reached. This approach presents as a simpler and more compact evaluation method compared to the local interpolation since just one iteration over boundary and domain is needed to calculate velocity derivatives.

5 NUMERICAL RESULTS

In this section the test performed for the direct boundary integral formulation implemented to predict slip behaviour for Couette and slit flow is presented, applying both interpolation approaches to the velocity derivatives in the shear rate used to evaluate the linear slip boundary condition.

5.1 Slit flow

The analytic solution for the velocity profile under slip flow over the horizontal surfaces is available in Matthews and Hill (2007):

$$u_1 = \frac{h^2}{2\mu}\frac{\Delta P}{L}\left[1-\left(\frac{x_2}{h}\right)^2\right] + \frac{h}{\mu}\frac{\Delta P}{L}L_s \tag{24}$$

where L is the channel length, h its height and ΔP the imposed pressure difference. The second term in the right side of equation (24) accounts the slip effect in the velocity profile. It reduces to no slip when L_s is dropped to zero as presented in Currie (2003). The tested mesh consisted of 320 quadratic elements on the outer surface refined at a the corners and 1911 internal collocation points.

For the local interpolation the velocity gradients are evaluated with information related to a finite amount of nodes near to the boundary nodes. A variation in the approaching ratio, R, means a variation on the amount of nodes available for velocity gradient evaluation and then in the accuracy of this value (see Table 1). As can be seen in the results for L2 norm error using the local approach, the interpolation performed with the GTPS function presented the most accurate results showing that its precision increase as the distance R is augmented, meaning that a greater quantity of nodes are used to calculate the velocity derivatives in the shear strain expression. The other RBFs used present errors over 12% while the approach through the GTPS has errors below 1% through the different distances used. It is also possible to notice, that a further increase in the approaching ratio to select the nodes has a negative influence on results achieved and showing that with a value equal to half the height of the separations between the plates ($R = 0.12$) the lowest L2 error is obtained.

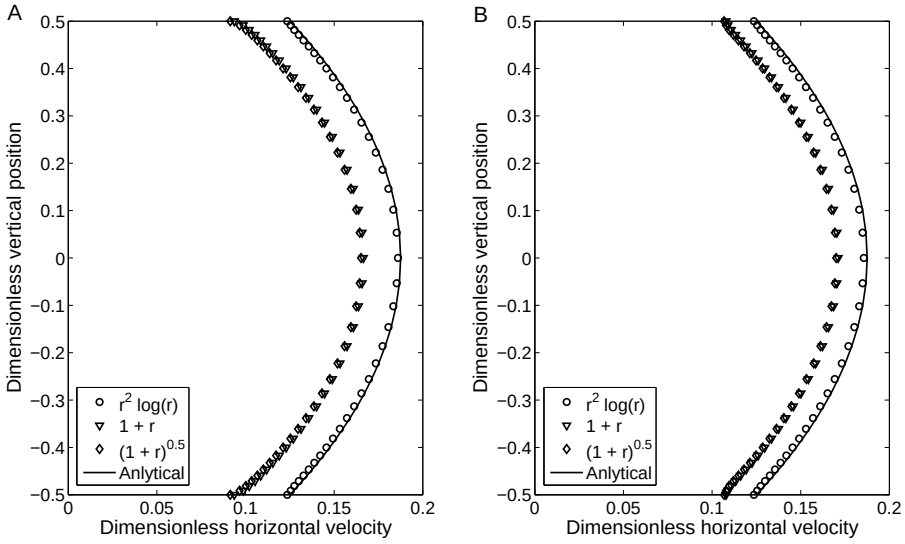

Figure 1: Velocity profiles for slip slit flow approaching shear rate with local (A) (approaching ratio $R = 0.12$) and global (B) interpolation approaching. $L_s = 0.5$

In respect to the global interpolation, the results in Table 1 present a similar behaviour that those for the local interpolation, showing that the GTPS function tends to allow more accurate results than the other two interpolation function tested. In Figure 1 results for both approaches using the three interpolation functions are plotted. The results shown in that figure correspond to a linear slip length, L_s, equal to 0.5 and an approaching ratio R of 0.12 in the case of the local interpolation. It is possible to observe that both approach with GTPS can accurately predict the velocity profiles in mixed boundary like the slit flow is.

Table 1: L2 norm error ($\%$) for slit flow under slip conditions

Local interpolation

	RBF		
R	r^2logr	$1+r$	$\sqrt{r+1}$
0.045	1.01	34.95	35.20
0.06	0.96	26.40	26.79
0.08	0.92	24.08	24.53
0.1	0.93	22.15	22.644
0.12	0.91	19.80	20.37
0.15	0.91	18.45	19.06
0.2	0.91	16.55	17.23
0.25	0.93	15.36	16.11
0.5	0.94	12.92	13.80

Global interpolation

RBF		
r^2logr	$1+r$	$\sqrt{r+1}$
1.045	10.19	10.94

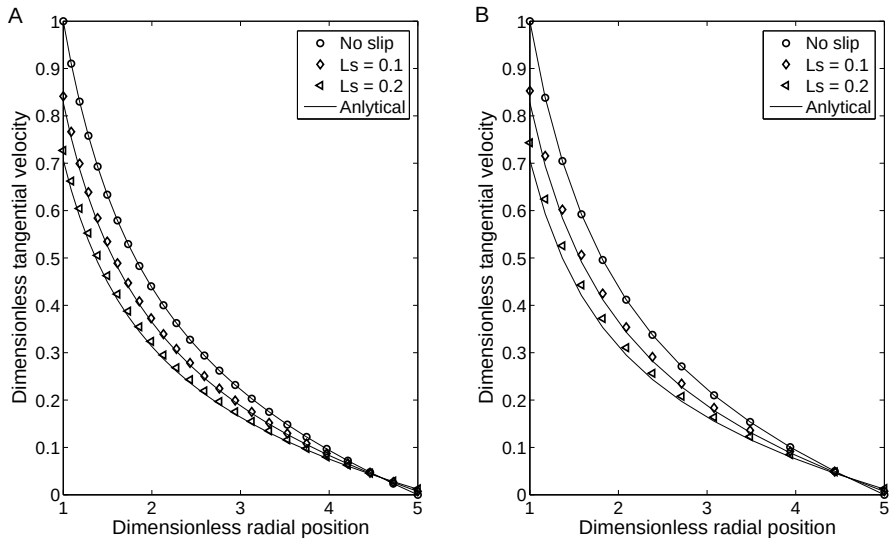

Figure 2: Velocity profiles for slip Couette flow where shear rate is approaching with GTPS (A) and $1 + r$ (B) global interpolation

5.2 Couette flow

An analytic solution for the tangential fluid velocity in Couette flow under linear slip boundary conditions is given by Barber et al. (2004):

$$u_t = \frac{\omega}{A - B}\left(Ar - \frac{1}{r}\right) \tag{25}$$

where

$$A = \frac{1}{r_e^2}\left(1 - 2\frac{L_s}{r_e}\right); \quad B = \frac{1}{r_i^2}\left(1 + 2\frac{L_s}{r_i}\right) \tag{26}$$

and being ω, r_e and r_i, the angular velocity for internal cylinder, external and internal radius, respectively. Tangential velocity u_t is given for any radius r. The slip length L_s variates between zero (no slip condition) and 1.0 to account for momentum transport variation at both the internal and external cylinders. When L_s is dropped to zero in equation (25), it reduces to Couette flow for no slip conditions as is presented in Currie (2003).

For the simulation of Couette flow under liner slip boundary conditions three meshes were used to check the effect of nodal densities over both boundaries and interior domain on numerical results. $Mesh\ 1$ and $Mesh\ 2$ have 2208 uniformly distributed internal points and 64 and 48 quadratic elements on both boundary surfaces, respectively. Meanwhile, the $Mesh\ 3$ has 48 quadratic elements on both boundary surfaces and 528 uniformly distributed internal points.

The results for slip flow evaluated with global interpolation are in Table 2. It can be observed that the GTPS function presents the lowest L2 norm errors compared with the other two RBF tested. Also, the effect of domain point densities could be observed as $Mesh\ 1$ and $Mesh\ 2$ present errors below 1%, while for the $Mesh\ 3$ errores are up to 3.8%. Meanwhile any further increase in the elements over boundary surface does not imply a significant improvement in the numerical results when error leves for $Mesh\ 1$ and $Mesh\ 2$ are compared. In the Figure 2 the results for global interpolation using GTPS and $1 + r$ functions are ploted. It is possible to

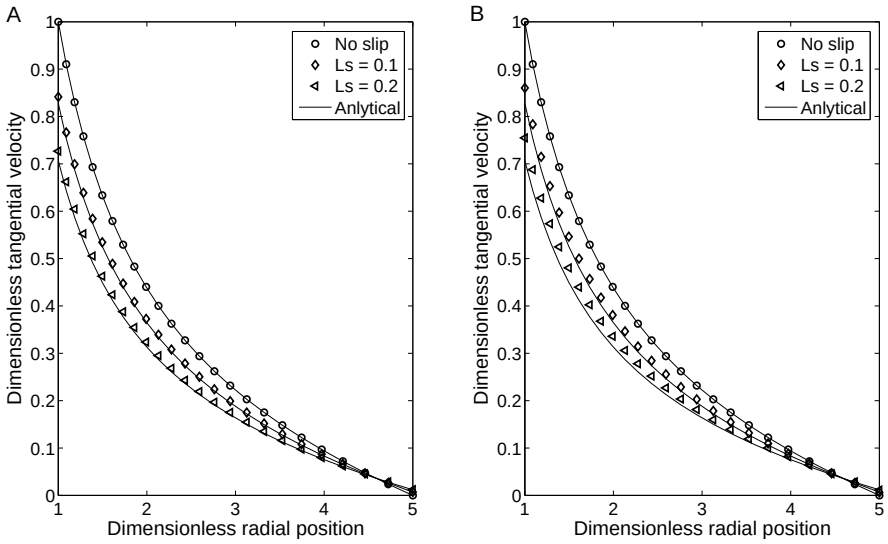

Figure 3: Velocity profiles for slip Couette flow where shear rate is approaching by GTPS local interpolation with $Mesh\ 1$ (A) and $Mesh\ 3$ (B)

Table 2: L2 norm error (%) for Couette flow under slip conditions - Global interpolation

$Mesh\ 1$			
R	$r^2 logr$	$1+r$	$\sqrt{r+1}$
$No\ slip$	0.001	0.001	0.001
$L_s = 0.1$	0.64	1.99	1.52
$L_s = 0.2$	1.13	2.61	2.66
$Mesh\ 2$			
R	$r^2 logr$	$1+r$	$\sqrt{r+1}$
$No\ slip$	0.002	0.002	0.002
$L_s = 0.1$	0.65	1.51	1.55
$L_s = 0.2$	1.13	2.66	2.71
$Mesh\ 3$			
R	$r^2 logr$	$1+r$	$\sqrt{r+1}$
$No\ slip$	0.002	0.002	0.002
$L_s = 0.1$	1.21	2.09	2.13
$L_s = 0.2$	2.11	3.71	3.79

Table 3: L2 norm error (%) for Couette flow under slip conditions - Local interpolation

	$R = 1.5$			$R = 2.5$			$R = 3.5$		
	$Mesh\ 1$								
RBF	r^2logr	$1+r$	$\sqrt{r+1}$	r^2logr	$1+r$	$\sqrt{r+1}$	r^2logr	$1+r$	$\sqrt{r+1}$
$No\ slip$	0.0015	0.0015	0.0015	0.0015	0.0015	0.0015	0.0015	0.0015	0.0015
$L_s = 0.1$	0.6	1.34	1.38	0.66	1.5	1.53	0.65	1.51	1.54
$L_s = 0.2$	1.11	2.33	2.39	1.16	2.63	2.68	1.15	2.65	2.69
	$Mesh\ 2$								
RBF	r^2logr	$1+r$	$\sqrt{r+1}$	r^2logr	$1+r$	$\sqrt{r+1}$	r^2logr	$1+r$	$\sqrt{r+1}$
$No\ slip$	0.0022	0.0022	0.0022	0.0022	0.0022	0.0022	0.0022	0.0022	0.0022
$L_s = 0.1$	0.59	1.38	1.43	0.64	1.55	1.59	0.65	1.57	1.6
$L_s = 0.2$	1.05	2.41	2.47	1.14	2.72	2.78	1.15	2.75	2.8
	$Mesh\ 3$								
RBF	r^2logr	$1+r$	$\sqrt{r+1}$	r^2logr	$1+r$	$\sqrt{r+1}$	r^2logr	$1+r$	$\sqrt{r+1}$
$No\ slip$	0.0022	0.0022	0.0022	0.0022	0.0022	0.0022	0.0022	0.0022	0.0022
$L_s = 0.1$	1.09	1.85	1.97	1.24	2.08	2.11	1.26	2.09	2.12
$L_s = 0.2$	1.93	3.27	3.35	2.16	3.69	3.75	2.56	3.71	3.77

observe how the $1+r$ fails to predict the velocity derivates at the boundaries understiamiting the velocity values respect to the analytic solution whilst the GTPS function succedes in predicting the velocty distribution for the no slip and the L_s range evaluated.

The L2 norm error results for local interpolation are in Table 3. In a similar way like with the slit flow the errors present a similar behaviour for the Couette flow when both interpolation approaches are compared. The GTPS function, like in the global interpolation, presents the more accurate results when local interpolation is used to evaluate the tangential projection of the shear rate in the slip boundary condition. Additionally, the use of dense domain meshes ($Mesh\ 1$ and $Mesh\ 2$) allows more precise result but no significant differences are observed when the boundary mesh is refined. Finally, the variation in the approaching ratio, R, do not significantly affect the results in terms of error levels while doing so in terms of computational cost due to increase in the number of nodes to evaluate the velocity gradients at each source node. Figure 3 shows the results for Couette flow obtained by using the GTPS function with an approaching ratio $R = 2.5$ for $Mesh\ 1$ and $Mesh\ 3$ in which is possible to observe the effect of domain mesh on velocity profiles.

6 CONCLUSIONS

A direct boundary integral method was used to evaluate slip flow behaviour for two traditional fluid flow problems. The linear slip boundary condition was used to link the velocity discontinuity at solid-fluid interface. The tangential projection of shear rate in the slip boundary condition was evaluated by implementing local and global interpolation with RBFs. Accurate results are obtained for both problems with both interpolation approaches when compared with analytic velocity profiles, being the more accurate results those obtained with the GTPS function. Additionally, the approach under both interpolation schemes allows to predict fluid flow behaviour in mixed boundary problems (slit flow) and shear rate boundary problems (Couette flow).

It is important to point out that, contrary to traditional BEM solutions, the internal nodes densities affect the solution of the problem due to dependency on the velocity derivatives accuracy

and the slip velocity evaluation on the amount of nodes used at the domain in both types of interpolation. In this way, even though all integrals in the formulation remain boundary integrals, the BEM partially lost its boundary-only nature and the dependence upon the amount of required domain nodes to achieve accuracy results finally translates in a higher computational cost. In two works recently presented by the authors, (Nieto et al., 2009a) and (Nieto et al., 2009b), the consideration of the slip behaviour avoids the use of RBF for the inclusion of Navier's boundary condition. In those works, the linear slip boundary condition was considered by expressing equation (1) as function of the vector surface traction $\vec{f}$ in the integral formulae for Stokes flow (5). The consideration of the slip flow in this way does not imply a dependency on domain nodes to the evaluation of shear rates in the boundary condition, allowing to more accurate results and less computational cost when compared with the RBF approach. Further work in the study of slip flow with the BEM will be held with the formulations developed in the works cited previously, despite the precision of the results obtained based on the RBF approach as presented in the actual work.

REFERENCES

Alvarado J., Mireles J., and Soriano G. Development and characterization of a capacitance-based microscale flowmeter. *Flow Measurement and Instrumentation*, 20:81–84, 2009.

Barber R., Sun Y., Gu X., and Emerson D. Isothermal slip flow over curved surfaces. *Vacuum*, 76:73–81, 2004.

Bird G. *Molecular gas dynamics and direct simulation of gas flows*. Oxford University Press, 1994.

Bothe D., Stemich C., and Warnecke H. Fluid mixing in a t-shaped micro-mixer. *Chemical Engineering Science*, 61:2950–2958, 2006.

Brebbia C. and Dominguez J. *Boundary Elements: An Introductory Course*. Computationanl Mechanics Publications, 1992.

Currie I. *Fundamental Mechanics of Fluids*. Macerl Dekker, 2003.

Flórez W. and Power H. Multi-domain dual reciprocity for the solution of inelastic non-Newtonian problems. *Computational Mechanics*, 27:396–411, 2001.

Gad-el Hak M. Gas and liquid transport at the microscale. *Heat Transfer Engineering*, 27:1–17, 2006a.

Gad-el Hak M. *MEMS: Applications*. CRC Press, 2006b.

Giraldo M., Ding Y., and Williams R. Boundary integral study of nanoparticle flow behaviour in the proximity of a solid wall. *Journal of Physics D: Applied Physics*, 41:1–10, 2008.

Giraldo M., Power H., and Flórez W. Mobility of shear thinning viscous drops in a shear Newtonian carrying flow using DR-BEM. *International Journal for Numerical Methods in Fluids*, 59:1321–1349, 2009.

Hu G. and Li D. Multiscale phenomena in microfluidics and nanofluidics. *Chemical Engineering Science*, 62:3443–3454, 2007.

Karniadakis G., Beskok A., and Aluru N. *Microflows and Nanoflows: Fundamentals and Simulation*. Springer, 2005.

Kleinstreuer C., Li J., and Koo J. Microfluidics of nano-drug delivery. *International Journal of Heat and Mass Transfer*, 51:5590–5597, 2008.

Lee H., Jeong Y., Shin J., Baek J., Kang M., and K. C. Package embedded heat exchanger for stacked multi-chip module. *Sensors and Actuators A: Physical*, 114:204–211, 2004.

Li X., Le Pierres R., and Dewson S. Heat exchangers for the next generation of nuclear reactors. In *Procedings on International Congress on Advances in Nuclear Power Plants*, pages 201–

209. 2006.

Luo H. and Pozrikidis C. Effect of surface slip on Stokes flow past a spherical particle in infinite fluid and near a plane wall. *Journal of Engineering Mathematics*, 62:1–21, 2008.

Matthews M. and Hill J. Newtonian flow with nonlinear Navier boundary condition. *Acta Mechanica*, 191:195–217, 2007.

Nguyen N. and Wereley S. *Fundamentals and Applications of Microfluidics*. Artech House, 2006.

Nieto C., Giraldo M., and Power H. Boundary integral method for Stokes flow with linear slip flow conditions in curved surfaces. In *Proceeding on 31st International Conference on Boundary Elements and Other Mesh Reduction Methods*, pages 353–362. 2009a.

Nieto C., Giraldo M., and Power H. Direct boundary integral formulation based on normal-tangential coordinates to evaluate slip flow over curved surfaces. In *Proceedings on Seventh UK conference on Boundary Integral Methods*, pages 151–160. 2009b.

Power H. and Wrobel L. *Boundary Integral Methods in Fluid Mechanics*. Computational Mechanics publications, 1995.

Sadus R. *Molecular simulation of fluids: Theory, applications and object-orientation*. Elsevier, 1999.

Shui L., Eijkel J., and van den Berg A. Multiphase flow in micro- and nanochannels. *Sensors and Actuators B: Chemical*, 121:263–276, 2007.

Telles J. A self-adaptative coordinate transformation for efficient numerical evaluation of general boundary element integrals. *International Journal for Numerical Methods in Engineering*, 24:959–973, 1987.

Thompson P. and Troian S. A general boundary condition for liquid flow at solid surfaces. *Nature*, 389:360–362, 1997.

Tonkovich A., Perrya S., Wangb Y., Qiua D., La Plantea T., and Rogersa W. Microchannel process technology for compact methane steam reforming. *Chemical Engineering Science*, 22:4819–4824, 2004.

Won Cha S., O'Hayre R., and Prinz F. The influence of size scale on the performance of fuel cells. *Solid State Ionics*, 175:789–795, 2004.